



Simultaneous Noncontact Precision Imaging of Microstructural and Thickness Variation in Dielectric Materials Using Terahertz Energy

Don J. Roth
Glenn Research Center, Cleveland, Ohio

Jeffrey P. Seebo
Lockheed Martin Space Systems Company, Hampton, Virginia

William P. Winfree
Langley Research Center, Hampton, Virginia

NASA STI Program . . . in Profile

Since its founding, NASA has been dedicated to the advancement of aeronautics and space science. The NASA Scientific and Technical Information (STI) program plays a key part in helping NASA maintain this important role.

The NASA STI Program operates under the auspices of the Agency Chief Information Officer. It collects, organizes, provides for archiving, and disseminates NASA's STI. The NASA STI program provides access to the NASA Aeronautics and Space Database and its public interface, the NASA Technical Reports Server, thus providing one of the largest collections of aeronautical and space science STI in the world. Results are published in both non-NASA channels and by NASA in the NASA STI Report Series, which includes the following report types:

- **TECHNICAL PUBLICATION.** Reports of completed research or a major significant phase of research that present the results of NASA programs and include extensive data or theoretical analysis. Includes compilations of significant scientific and technical data and information deemed to be of continuing reference value. NASA counterpart of peer-reviewed formal professional papers but has less stringent limitations on manuscript length and extent of graphic presentations.
- **TECHNICAL MEMORANDUM.** Scientific and technical findings that are preliminary or of specialized interest, e.g., quick release reports, working papers, and bibliographies that contain minimal annotation. Does not contain extensive analysis.
- **CONTRACTOR REPORT.** Scientific and technical findings by NASA-sponsored contractors and grantees.

- **CONFERENCE PUBLICATION.** Collected papers from scientific and technical conferences, symposia, seminars, or other meetings sponsored or cosponsored by NASA.
- **SPECIAL PUBLICATION.** Scientific, technical, or historical information from NASA programs, projects, and missions, often concerned with subjects having substantial public interest.
- **TECHNICAL TRANSLATION.** English-language translations of foreign scientific and technical material pertinent to NASA's mission.

Specialized services also include creating custom thesauri, building customized databases, organizing and publishing research results.

For more information about the NASA STI program, see the following:

- Access the NASA STI program home page at <http://www.sti.nasa.gov>
- E-mail your question via the Internet to help@sti.nasa.gov
- Fax your question to the NASA STI Help Desk at 301-621-0134
- Telephone the NASA STI Help Desk at 301-621-0390
- Write to:
NASA Center for AeroSpace Information (CASI)
7115 Standard Drive
Hanover, MD 21076-1320



Simultaneous Noncontact Precision Imaging of Microstructural and Thickness Variation in Dielectric Materials Using Terahertz Energy

Don J. Roth
Glenn Research Center, Cleveland, Ohio

Jeffrey P. Seebo
Lockheed Martin Space Systems Company, Hampton, Virginia

William P. Winfree
Langley Research Center, Hampton, Virginia

National Aeronautics and
Space Administration

Glenn Research Center
Cleveland, Ohio 44135

Level of Review: This material has been technically reviewed by technical management.

Available from

NASA Center for Aerospace Information
7115 Standard Drive
Hanover, MD 21076-1320

National Technical Information Service
5285 Port Royal Road
Springfield, VA 22161

Available electronically at <http://gltrs.grc.nasa.gov>

Simultaneous Noncontact Precision Imaging of Microstructural and Thickness Variation in Dielectric Materials Using Terahertz Energy

Don J. Roth
National Aeronautics and Space Administration
Glenn Research Center
Cleveland, Ohio 44135

Jeffrey P. Seebo
Lockheed Martin Space Systems Company
Hampton, Virginia 23681

William P. Winfree
National Aeronautics and Space Administration
Langley Research Center
Hampton, Virginia 23681

Abstract

This article describes a noncontact single-sided terahertz electromagnetic measurement and imaging method that simultaneously characterizes microstructural (egs. spatially-lateral density) and thickness variation in dielectric (insulating) materials. The method was demonstrated for two materials—Space Shuttle External Tank sprayed-on foam insulation and a silicon nitride ceramic. It is believed that this method can be used as an inspection method for current and future NASA thermal protection system and other dielectric material inspection applications, where microstructural and thickness variation require precision mapping. Scale-up to more complex shapes such as cylindrical structures and structures with beveled regions would appear to be feasible.

Introduction

The Columbia Accident Investigation Board recommendation R3.2.1 stated “Initiate an aggressive program to eliminate all External Tank Thermal Protection System debris-shedding at the source....” To support this recommendation, inspection methods for flaws in foam are being evaluated, developed, and refined at NASA. Terahertz c-scan imaging is an emerging and very effective nondestructive evaluation (NDE) technique used for dielectric materials analysis and quality control in the pharmaceutical, biomedical, security, materials characterization, and aerospace industries. Background information and results with terahertz measurements can be obtained from several references (Altan, et al., 2004; Ammone et al., 1999; Hu and Nuss, 1995; Mittleman, et al.; 1996, Mittleman, et al.; 1999; Roth et al. 2006; Winfree and Madaras, 2005). Briefly, terahertz waves are electromagnetic waves with wavelengths on the order of 200 to 1000 μm . Reflections occur to varying degree at interfaces between materials with dissimilar dielectric properties (difference in indices of refraction). Metallic materials totally reflect terahertz waves while nonpolar liquids, dielectric solids, and gases are at least partially transparent to terahertz energy. Continuous wave (narrowband) and pulsed (broadband) terahertz systems exist. This study is based on results from a reflection-mode broadband terahertz method with a collinear source-detector (transceiver) configuration shown schematically in figure 1.

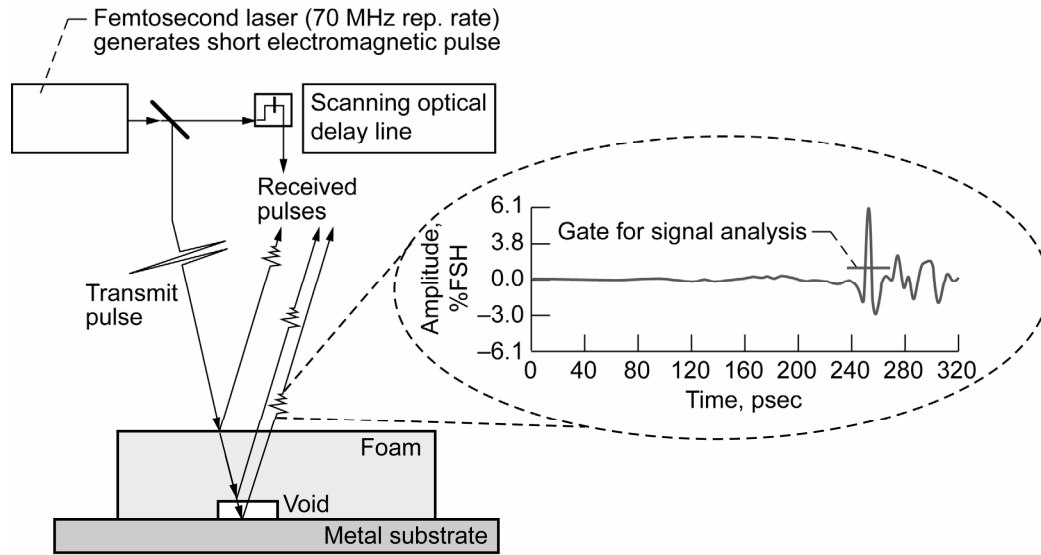


Figure 1.—Basic schematic diagram of reflection-mode terahertz methodology. Reflections will be received off of the various interfaces. Reflection from metal will be the strongest. The horizontal dotted line over the echo shows the time gate typically used during signal processing.

Terahertz imaging is being used at NASA for nondestructive evaluation of the Space Shuttle external tank thermal protection system sprayed-on foam insulation (SOFI). Generally, it is used in the pulse-echo c-scan configuration to map variations in the peak amplitude of the echo off of the metal substrate (equivalent to the location of the back surface of the foam) that occur when scanning across a section of foam in order to detect voids, cracks, disbonds, and any sort of discontinuity. Traditional c-scan imaging scales the peak amplitude values (to an 8- or 16-bit gray or color scale) at each scan location to form an image.

An additional implementation of pulse-echo c-scan imaging involves mapping variations in the time-of-flight of a terahertz echo peak, or mapping the time delay between front and substrate (with the sample present) echoes. This implementation concerns itself more with mapping thickness or global microstructural variation (such as physical density variation) as opposed to discrete flaw detection. Time delay between the front surface echo and substrate echo (with the sample present) (2τ) is directly affected by thickness variation (d) and terahertz velocity (V) in the material according to:

$$2\tau = \frac{(2d)}{V} \quad (1)$$

Here the designations 2τ and $2d$ (versus τ and d) are used since the ultrasonic echo travels through twice the material thickness in the pulse-echo mode. Terahertz velocity is affected by variations in a volumetric microstructural property such as physical density (fig. 2), similar to the way ultrasonic velocity responds to microstructural variation (Generazio et al., 1989, Roth et al., 1991, Roth et al., 1995). Determining the relationship between velocity and density allows actual density maps to be obtained from velocity maps as will be demonstrated in this article.

Spatial variations in part thickness and/or spatially-lateral microstructural character will result in variations in maps of 2τ . Analogous to a complex number having real and imaginary parts, 2τ images can be thought of as having thickness and microstructural components if both thickness and microstructural variation are present. This study presents a terahertz method which allows the separation of time-of-flight variations into its microstructural and thickness components. This method becomes important in order to correctly determine the extent of microstructural variation in a part that also has thickness variation. Additionally, it provides a noncontact method for mapping thickness and/or density in parts.

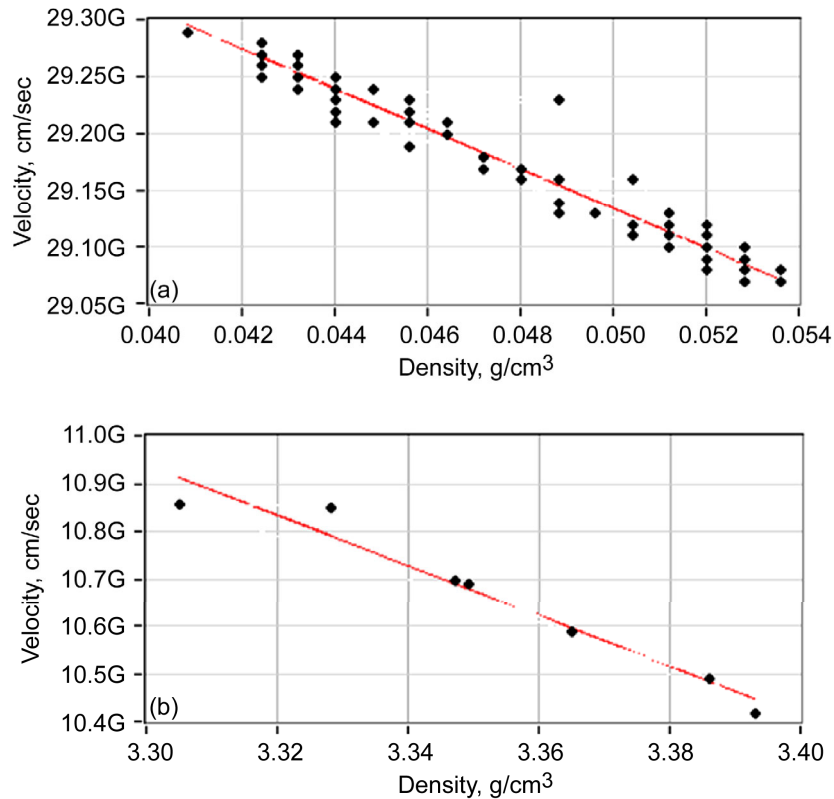


Figure 2.—Terahertz velocity versus physical density including best linear curve fit. (a) Terahertz velocity versus density for external tank sprayed-on foam insulation derived by using the mean of 300 to 400 velocity data points for 77 foam cubes. (b) Terahertz velocity versus density for silicon nitride using terahertz velocity and percent porosity at selected points on silicon nitride sample (theoretical density = 3.44 g/cm³). G = 10⁹.

Prior Art

Several attempts to separate thickness and microstructural variation effects in ultrasonic images were noted (Bashyam, 1991). (Bashyam, 1991) used a two-transducer ultrasonic method whereby the transducers were used in both pulse-echo and through-transmission mode to monitor thickness via time-of-flight information and track echo peak amplitude. Knowing the thickness at each scan location, the material attenuation coefficient, and the assumption that the attenuation coefficient is constant throughout the part, a c-scan image can be produced free of thickness effects. Several references showed single point (nonimaging) ultrasonic measurement methodology that accounted for thickness variation effects (Hsu, et al., 1994 and Piche', 1984). (Hsu et al., 1994) simultaneously determined ultrasonic velocity, plate thickness and wedge angle with a method that conceivably could be extended to imaging. (Sollish, 1977; Piche', 1984) described a single point ultrasonic velocity measurement method using a reflector plate located behind the sample that does not require prior knowledge of sample thickness and lends itself to multiple measurements within a sample of nonuniform thickness. Several references proceeded to scale up and automate this ultrasonic method to obtain ultrasonic velocity images for plate and cylindrical samples of various materials of nonuniform thickness (Dayal et al., 1994; Roth et al., 1996; Roth et al., 1997; Roth et al., 1998; Roth et al., 2000).

No attempts to separate thickness and microstructural variation effects in terahertz time-of-flight images were noted in the literature. Terahertz methods to obtain thickness images of foam based on empirical relationships developed from attenuation as a function of thickness have been used but do not

account for microstructural variation (Trinh, 2006). A similar procedure could be envisioned to develop an empirical relationship between attenuation and density, but would not account for thickness variation. A procedure utilized in ultrasonics and terahertz in which the substrate reflector plate time-of-flight scan with no sample present is subtracted from the same scan with the sample in place is useful to characterize microstructure and correct for setup nonuniformity/nonlevelness, but will not separate thickness and microstructural effects (Seebo, 2006).

Methodology

In this investigation, the conventional terahertz method of inspecting metal reflector-backed dielectric materials is taken advantage of to simultaneously provide thickness-independent velocity (free of thickness effects) and microstructure-independent thickness (free of microstructure effects) images. Figure 3 shows a schematic of the pulse-echo terahertz testing method and resulting waveforms. A pulse-echo terahertz velocity measurement is made by sending terahertz energy via a transceiver (device that has both a transmitter and a receiver) into and through a dielectric (insulating) material backed by a plate (electrically-conducting, generally metallic) that reflects the terahertz energy back to the transceiver. The terahertz transceiver is separated from the dielectric sample by an air path.

The novel pulse-echo method described here for measuring velocity in a material sample uses echoes off of the reflector plate with (*BS*) and without the sample present (*M'*), as well as using the echo off of the sample front surface (*FS*). The following steps show how velocity (*V*) in a sample of thickness (*d*) is determined without needing prior knowledge of thickness. With a dielectric sample present between the transceiver and the reflector plate, the pulse that travels from the transceiver through the sample to the reflector plate (equivalent to the sample back surface position) and back to the transceiver is labeled *BS* and will be observed at time *t'* where:

$$t' = (2t_1 + 2\tau) \quad (2)$$

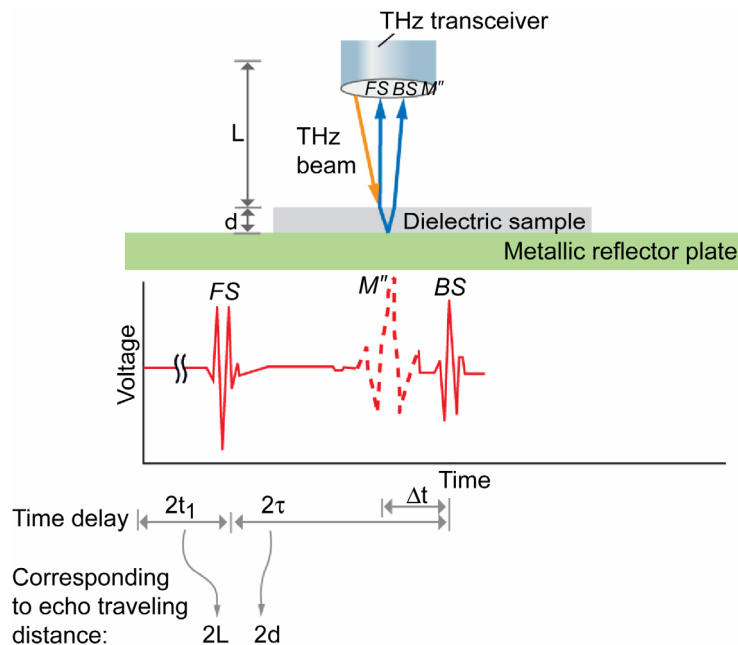


Figure 3.—Schematic of the pulse-echo terahertz testing and resulting waveforms. *FS* and *BS* occur with the sample present. *M'* occurs without the sample present. THz = terahertz.

where $2t_1$ and 2τ are the pulse-echo time delays of the terahertz pulse from the transceiver to the sample front surface and from the sample front surface to the substrate (with the sample present), respectively (fig. 3). Placing a dielectric sample in between the terahertz transceiver and the reflector plate slows down the terahertz pulse as compared to its travel time in air. Thus, with the sample removed, the pulse that travels from the transceiver to the reflector plate and back to the transceiver is labeled M'' and will be observed at an earlier time t'' where:

$$t'' = \left(2t_1 + 2\frac{d}{c} \right) \quad (3)$$

where c is the velocity of terahertz energy in air and d is the air gap equal to the sample thickness. The velocity of light at standard temperature and pressure was used for c in this investigation and is equal to 0.02997055434 cm/psec. Subtracting equation (3) from equation (2) gives:

$$t' - t'' = \Delta t = 2\tau - 2\frac{d}{c} \quad (4)$$

The thickness (d) of the sample can be determined in the pulse-echo configuration from:

$$2d = (2\tau)V \quad (5)$$

Solving equation (5) for d and substituting the result into equation (4) gives:

$$\Delta t = 2\tau - \frac{2\tau V}{c} \quad (6)$$

Rearranging equation (6) to solve for V gives:

$$V = c \left(1 - \frac{\Delta t}{2\tau} \right) \quad (7)$$

As seen from equation (7), sample thickness (d) is not a variable in the equation. Thus, this method does not require prior knowledge of sample thickness. If extended to multiple measurements across the sample (imaging), sample thickness variation effects are eliminated in the image allowing a true picture of microstructural variation for types of microstructural variation (such as density variation) that correlate with and will be revealed by velocity variation. For conventional time-of-flight imaging (eq. (1)), thickness variation effects would corrupt the evaluation of microstructural variation—thus the new methodology allows true characterization of microstructural variation in a material structure that is also nonuniformly thick. Equation (7) shows how the terahertz velocity in a dielectric material will be reduced fractionally from that in air by the factor:

$$\left(1 - \frac{\Delta t}{2\tau} \right) \quad (8)$$

Further, rearranging equation (4) to solve for sample thickness (d) gives:

$$d = \frac{c(2\tau - \Delta t)}{2} \quad (9)$$

which allows the calculation of absolute material thickness without prior knowledge of velocity. If extended to multiple measurements across the sample (imaging), sample microstructure variation effects are eliminated in the image allowing a true mapping of thickness variation. For conventional thickness mapping (rearrange eq. (1) to solve for (d)), microstructure variation effects would corrupt the evaluation of thickness variation—thus the new methodology allows true characterization of thickness variation in a material structure that is of nonuniform microstructure. A key point of the methodologies presented in this section are that both thickness-independent velocity and microstructure-independent thickness images can be derived from the same set of scan information.

In practice, 2τ is experimentally obtained from the pulse-echo time delay between the first front surface (FS) and substrate echo with the sample present (BS) (fig. 3). Either the time difference from FS peak location to BS peak location or cross-correlation (Hull, et al., 1985) of the two echoes can be used to obtain the 2τ time delay. Δt is the pulse-echo time difference between the echo off the reflector plate with and without the sample present, respectively.

Ramifications

Flaws present in the Space Shuttle external tank thermal protection system may play a role in foam release and are therefore important to detect and characterize prior to flight (CAIB report). The external tank configuration has sprayed-on foam insulation (SOFI) placed on top of the metal container and thus lends itself to terahertz inspection. Terahertz inspection has shown significant promise for detection of voids in the foam for metallic-backed SOFI test articles (Roth, et al., 2006) for. Other potentially undesirable foam anomalies that have been identified include density variations and crushed foam (NESC ET TPS NDE SPRT Final Report, 2007). In fact, after the shuttle flight STS-114, the ability to nondestructively detect crushed foam became a significant priority. The microstructure-independent thickness mapping method can be used to identify **and quantify** areas of crushed (pushed-in) foam and precisely map thickness. The thickness-independent velocity method can be used to identify **and quantify** density variations in foam and other materials. It is worth noting that the previously-discussed ultrasonic methods for thickness-independent velocity and microstructure-independent thickness (Sollish, 1977; Piche', 1984; Dayal, 1992; Roth et al., 1996) require water coupling while no such coupling is needed for terahertz methods. The latter fact makes the terahertz method much more practical than the ultrasonic method for dielectric materials.

Limitations

The front surface echo off of the dielectric material may be of very low signal-to-noise ratio (SNR) depending on the dielectric match between air and the sample. If a good dielectric match exists, much of the terahertz energy will be transmitted into the sample. Additionally, the focal plane sensitivity of the terahertz method for samples of nonuniform thickness may result in the FS echo too far out of focus and thus reduce SNR even further, thus limiting the thickness variation over which the method can be used. The approximate time location of FS must be known apriori and the wavetrain examined manually in the software oscilloscope trace in order to determine what special post-processing needs to be applied in order to amplify and denoise FS . For the space shuttle external foam, the FS echo can be as small as 1/100th the amplitude of the BS echo. This requires signal processing/conditioning steps of denoising and/or low-pass (smoothing) filtering followed by amplification (software gain) at the time location(s) of the FS echo to clearly separate the FS echo from baseline noise. Specific conditioning parameters will be described in the EXPERIMENTAL section. To create a better dielectric mismatch situation in which more of the terahertz energy is reflected back to the receiving system while an ample amount is still

transmitted into the sample, a sheet of very thin (250 μm) plastic transparency paper can be placed onto the sample. This method can be used to locate the front surface echo locations prior to scanning, or in situations where it can be tolerated during actual scanning, will provide front surface echoes of much greater SNR. Also, knowledge of distance between scanner head and sample top surface, velocity of terahertz in air (speed of light), and any post- or pre-trigger delays should allow calculation of approximate front surface time location(s). It should be noted that further studies to determine practical thickness variation limit are required.

Measurement Uncertainty

The precision (uncertainty) in the thickness-independent velocity (σ_V) due to the random errors in the measurements of the variables Δt , and 2τ was obtained by use of equation (7) and the variance relation (Bevington, 1969) to give (ignoring uncertainty in c):

$$\sigma_V^2 = \left(\frac{\partial V}{\partial(\Delta t)} \right)^2 (\sigma_{\Delta t})^2 + \left(\frac{\partial V}{\partial(2\tau)} \right)^2 (\sigma_{2\tau})^2 \quad (10)$$

where

$$\left(\frac{\partial V}{\partial(\Delta t)} \right) = -\frac{c}{2\tau}, \quad (11)$$

$$\left(\frac{\partial V}{\partial(2\tau)} \right) = \frac{c(\Delta t)}{(2\tau)^2}, \quad (12)$$

and

$$\sigma_{\Delta t} = \sigma_{\Delta 2\tau} = \left(\frac{1}{2 * SR} \right)$$

where SR = sampling rate and jitter is not considered. Percent uncertainty in the thickness-independent velocity is given by

$$U_V = \left(\left| \frac{\sigma_V}{V} \right| \right) 100 \quad (13)$$

Figure 4 shows %uncertainty U_V in thickness-independent velocity measurement as a function of Δt , 2τ , and V .

For the foam samples and the experimental setup of this study, given good quality initial or signal-processed waveforms, and using typical values of $\Delta t \sim 6$ psec, $2\tau \sim 200$ psec, $SR = 6.4$ THz, $c = 0.02997055434$ cm/psec, and $V \sim 0.0290$ cm/psec, gives $U_V \sim 0.01$ percent.

Similarly, the precision (uncertainty) in the microstructure-independent thickness (σ_d) is:

$$\sigma_d^2 = \left(\frac{\partial d}{\partial(\Delta t)} \right)^2 (\sigma_{\Delta t})^2 + \left(\frac{\partial d}{\partial(2\tau)} \right)^2 (\sigma_{2\tau})^2 \quad (14)$$

where

$$\left(\frac{\partial d}{\partial(\Delta t)} \right) = -\frac{c}{2} \quad (15)$$

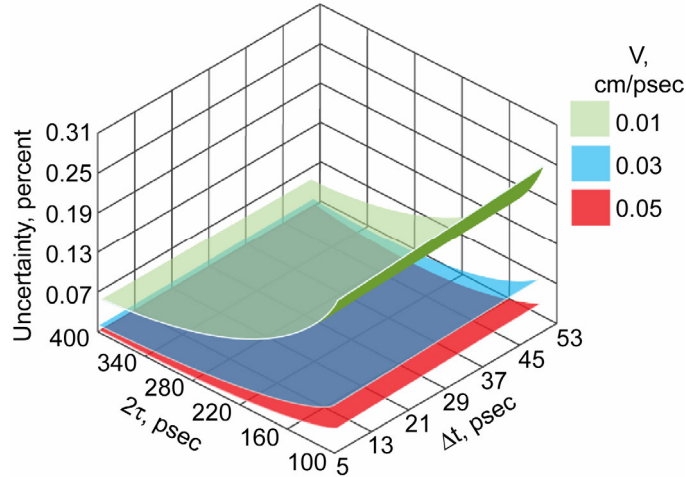


Figure 4.—Percent Uncertainty U_V in thickness-independent velocity measurement as a function of Δt , 2τ , and V for $V = 0.01, 0.03,$ and 0.05 cm/psec.

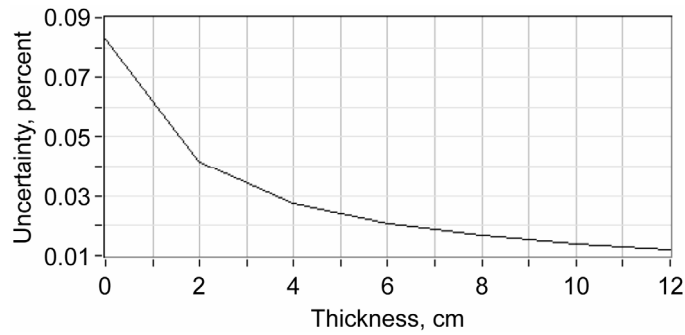


Figure 5.—Percent Uncertainty U_d in microstructure-independent velocity as a function of thickness.

and

$$\left(\frac{\partial d}{\partial(2\tau)} \right) = \frac{c}{2} \quad (16)$$

Percent uncertainty in the microstructure-independent thickness is given by

$$U_d = \left(\left| \frac{\sigma_d}{d} \right| \right) 100 \quad (17)$$

Since both partial derivatives (eqs. (15) and (16)) give constants, U_d is only dependent upon the value of thickness (fig. 5).

For the foam samples and the experimental setup of this study, given good quality initial or signal-processed waveforms, and using typical values $SR = 6.4$ THz, $c = 0.02997055434$ cm/psec, and $d \sim 3$ to 5 cm, gives $U_d = 0.035$ to 0.025 percent.

Experimental

Materials

Several sets of blocks of external tank thermal protection system foam were tested with the described terahertz method. The first set consisted of a 6 by 15 array of foam blocks of about 5 by 5 by 5 cm in dimensions with minor but nonregular thickness variation (± 0.1 cm). The blocks were of various densities ranging from about 0.042 to 0.054 g/cm³ (on the order of 20 percent) measured from mass and dimensional measurements and were arranged randomly. The next set of foam blocks scanned were trim cut from the 5 by 5 by 5 cm blocks such that thicknesses were reduced to between 3 to 4 cm to give sets of blocks of varying thickness and density. Since the foam spray process results in nonuniform density from the base layer to the top of the block, the densities were remeasured after cutting. Also, a rectangular foam sample about 12 cm in length was trim cut to form a smooth wedge. Several foam block configurations were investigated from the cut samples: the smooth wedge, and two sets of blocks having both density and thickness variation, but ordered as step wedges such that in one case density and thickness variation would result in additive effect on 2τ (Group A), and in the other case ordered such that density and thickness variation would have an opposing effect on 2τ (Group B). A ceramic silicon nitride sample was also scanned with the terahertz method and had a small density variation of 2 percent due to porosity variation, and had thickness variation machined in that was on the order of 10 percent (0.32 to 0.35 to 0.03 cm variation) (Roth et al., 1997). Some of the samples interrogated by the terahertz inspection method in this study are shown in figure 6.

Terahertz Experimental Setup

Table 1 describes the broadband 1 THz scan system and associated experimental parameters.

TABLE 1.—EXPERIMENTAL PARAMETERS FOR TERAHERTZ SCAN SYSTEM AND SIGNAL PROCESSING

Focus	At substrate, or 3 cm above substrate for wedge samples
Typical Received Bandwidth Points (THz) (Full Width Half Max)	~0.1 to 0.3
Data Acquisition Rate (THz)	6.4
Waveform Length Acquired (psec/points)	320 psec/2048 points
Waveform Acquisition Rate (scan points/sec)	~10
Collinear source-detector	Yes
Spatial Resolution (at Full Width Half Max of Point Spread Function) (cm)	0.5
Signal Acquisition: Width of dynamic (peak-centered) gates for time delay computations (psec)	25 to 100
Scan Increment (cm)	0.2
<i>FS</i> Conditioning (for foam)	Wavelet Denoising, 10 to 40x Amplification, DC subtraction

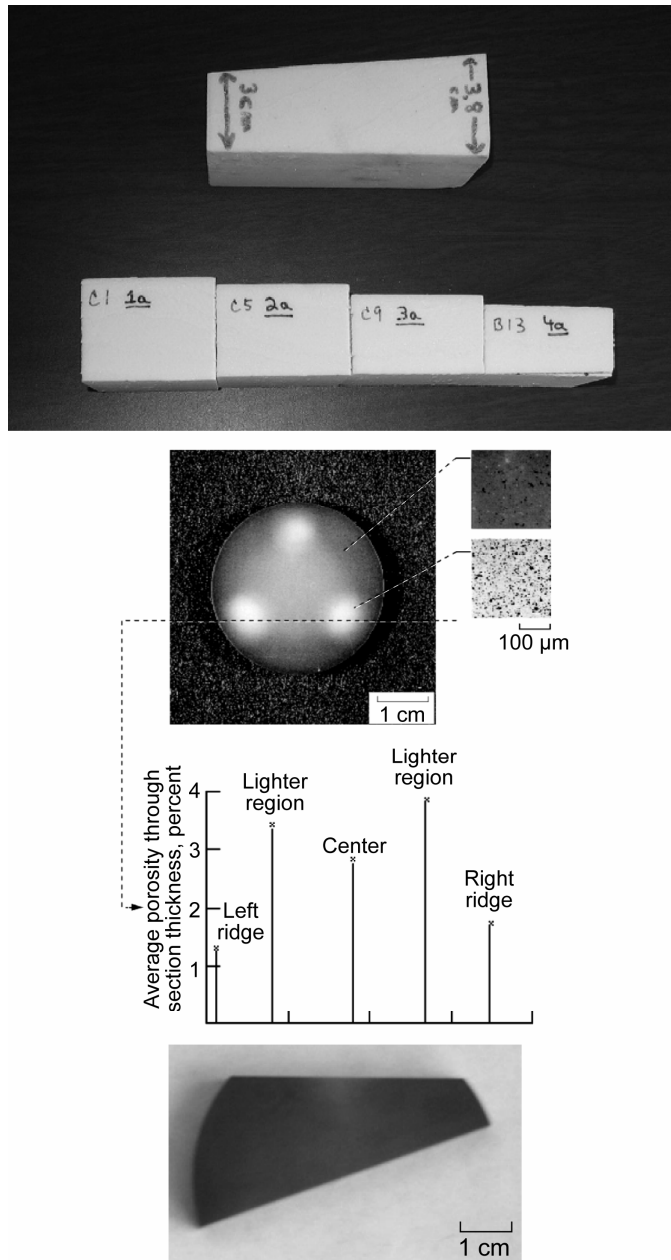


Figure 6.—Some of the samples interrogated by Terahertz inspection method. (a) Side view of a set of foam blocks (Group A) of different thickness and density (density variation not visible) and side view of foam block smooth wedge. (b) Ceramic silicon nitride wedge and disk from which the wedge was cut containing lower-than-average pockets of density and an edge-to-center density gradient. The wedge was machined to have a 0.03 cm thickness gradient from left-to-right edge.

Scanning

Samples were placed on an aluminum plate within the scan system hardware as shown in figure 7. Scan increment in the X and Y direction was 0.2 cm.

The minimum number of scans required to obtain thickness-independent velocity and microstructure-independent thickness is two so as to be able to obtain *FS* and *BS* echoes in one scan (with sample present), and *M'* echo (without sample present). Separate scans for *FS* and *BS* can be performed if sample thickness is too large to allow simultaneous capture of both of the echoes in the 320 psec/2048 point window using 6.4 THz sampling rate. In this study, only two scans were required when the thicknesses were ≤ 4 cm and *FS* and *BS* could be captured in one scan. For each sample set, the scans were then “fused” such that *FS*, *BS* and *M'* echoes were placed in a single wavetrain of 640 psec/4096 points length with time relationships between the echoes preserved (fig. 8). This occurs at each scan location to create the new fused data set. Precise time delays 2τ and Δt were determined using cross-correlation between echoes. Phase relationships were examined for 1) *FS* compared to *BS* and 2) *BS* compared to *M'*. For our present study, all waves appeared to be in phase. If echoes are in-phase with respect to each other, the time occurrence of the *maximum* in the correlation function was used to calculate time delay. (If the echoes were phase-inverted, the time occurrence of the *minimum* in the correlation function was to be used calculate time delay.)

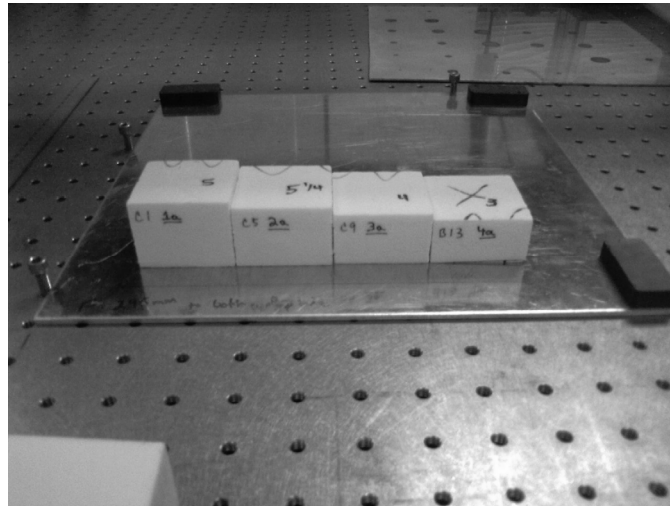


Figure 7.—Foam block sample set Group A placed on aluminum plate. Scan Head located above blocks is mounted on manipulators for X, Y, and Z movement.

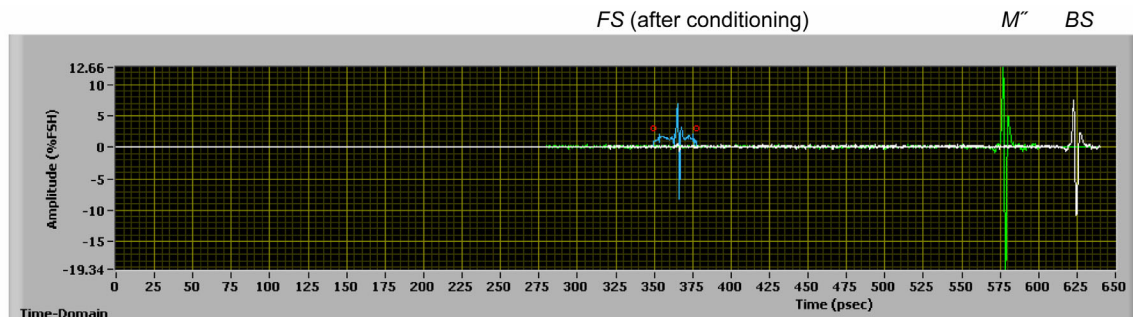


Figure 8.—A typical “fused” waveform from “fused” data file produced by merging the *FS*, *BS*, and *M'* scan data sets for foam block sets. *FS* and *BS* occur with the sample present. *M'* occurs without the sample present. For visualization purposes, *M'* has been artificially shifted to the left an additional 40 psec to avoid overlap between the echoes for visualization purposes. *FS* has been denoised, amplified, and had DC component subtracted so as to allow 2τ time delay calculation.

Signal Conditioning

For this study, a 25 to 100 psec gate (window) was applied to account for variations in front surface echo position due to thickness variations. The gated region containing the *FS* echo is denoised using a wavelet process, then amplified by 10 to 40x, followed by subtraction of the DC component. The denoising process used the debauchies 05 mother wavelet (Jensen, 2001). The resultant *FS* echo was quite useable as shown in figure 8.

Results

Group A Step Wedge With Known Thickness and Density Variation Pattern

Figure 9 shows 2τ , microstructure-independent thickness, and density images from the terahertz method for the Group A step wedge foam block set. The density image was derived from thickness-independent velocity image using relationship between terahertz velocity and density for foam shown in figure 2(a). This sample has well-defined thickness and density variation that have additive effects on the 2τ image. It can be seen that the method is able to separate the thickness and density variation components.

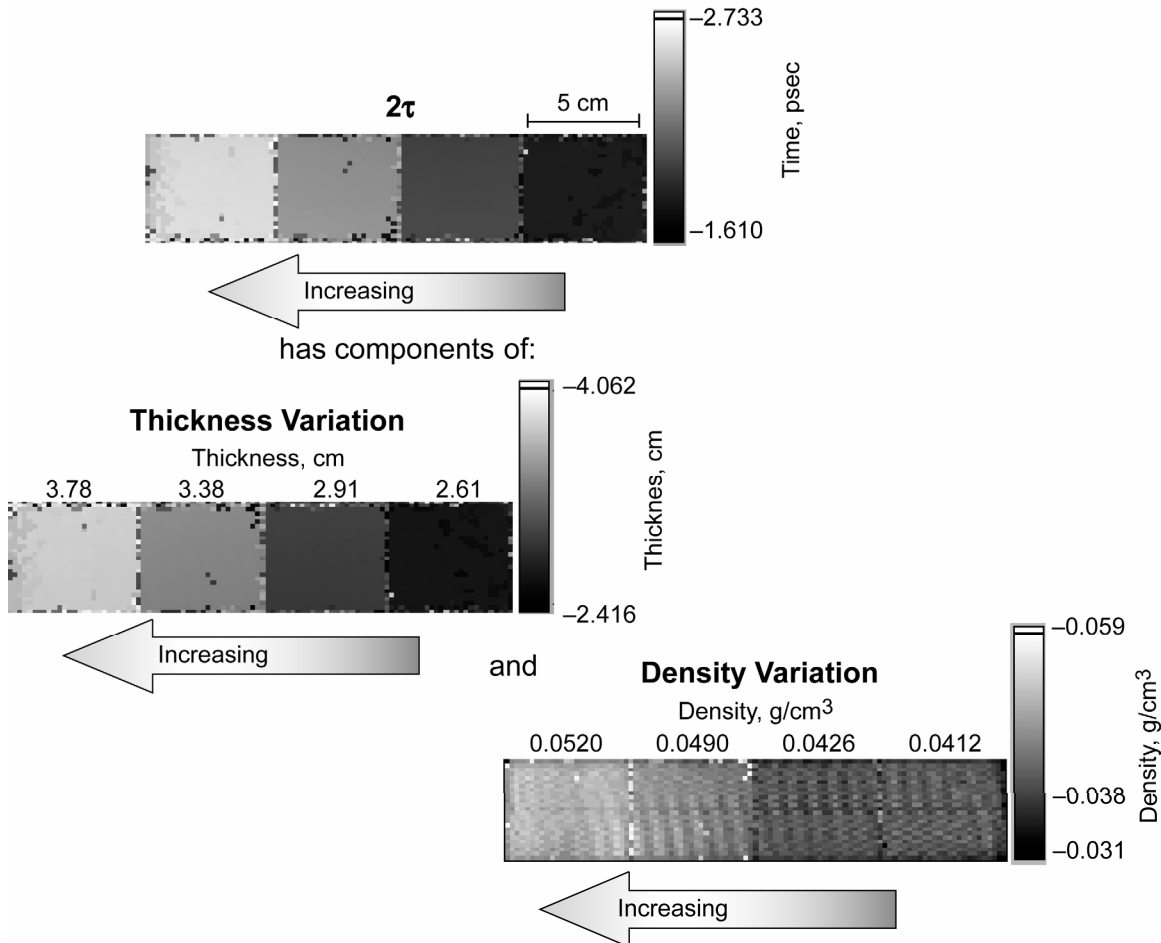


Figure 9.—Results for Group A Foam Blocks from terahertz method. Method can be seen to separate out thickness and density effects on time delay (2τ) between *FS* and *BS* echoes. Increasing thickness and increasing density from right-to-left in blocks provides an additive effect in terms of increasing 2τ from right-to-left. Scan and/or analog-to-digital conversion jitter (zigzag gray level pattern) is apparent in the density image of this and following figures.

Group B Step Wedge With Known Thickness and Density Variation Pattern

Figure 10 shows 2τ , microstructure-independent thickness, and density images from the terahertz method for the Group A step wedge foam block set. The density image was derived from thickness-independent velocity image using relationship between terahertz velocity and density for foam shown in figure 2(a). This sample has well-defined thickness and density variation that have opposing effects on the 2τ image. It can be seen that the method is able to separate the thickness and density variation components. The 2τ image is dominated by the thickness variation.

Smooth Foam Wedge With Known Thickness Variation and Unknown Density Variation

Figure 11 shows 2τ , microstructure-independent thickness, and density images from the terahertz method for the smooth foam wedge. The density image was derived from thickness-independent velocity image using the relationship between terahertz velocity and density for foam shown in figure 2(a). It can be seen that the 2τ image clearly reflects the thickness variation seen in the thickness image. Some minor

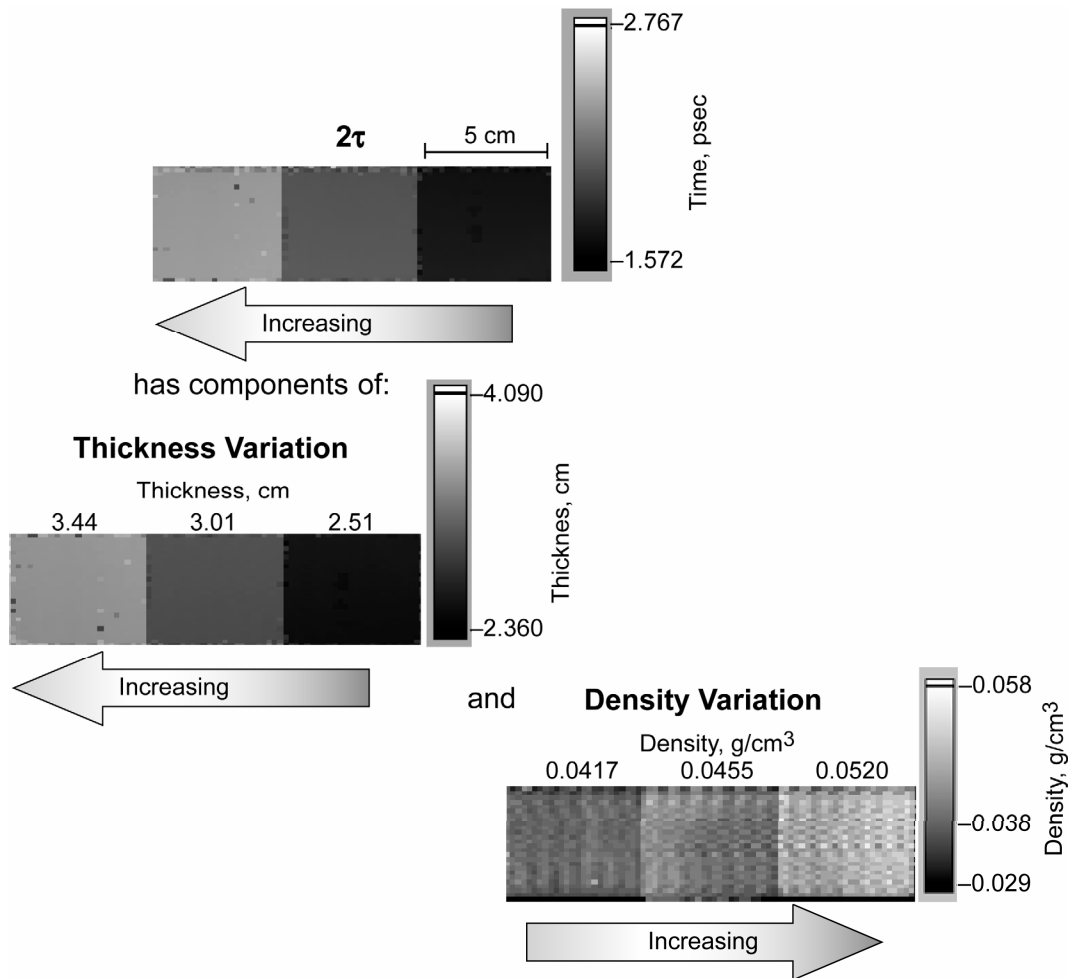


Figure 10.—Results for Group B Foam Blocks. Method can be seen to separate out thickness and density effects on time delay (2τ) between *FS* and *BS* echoes. Density image was derived from thickness-independent velocity image using relationship between terahertz velocity and density for foam shown in figure 2(a). Increasing thickness from right-to-left and increasing density from left-to-right in blocks provides opposing effects on 2τ .

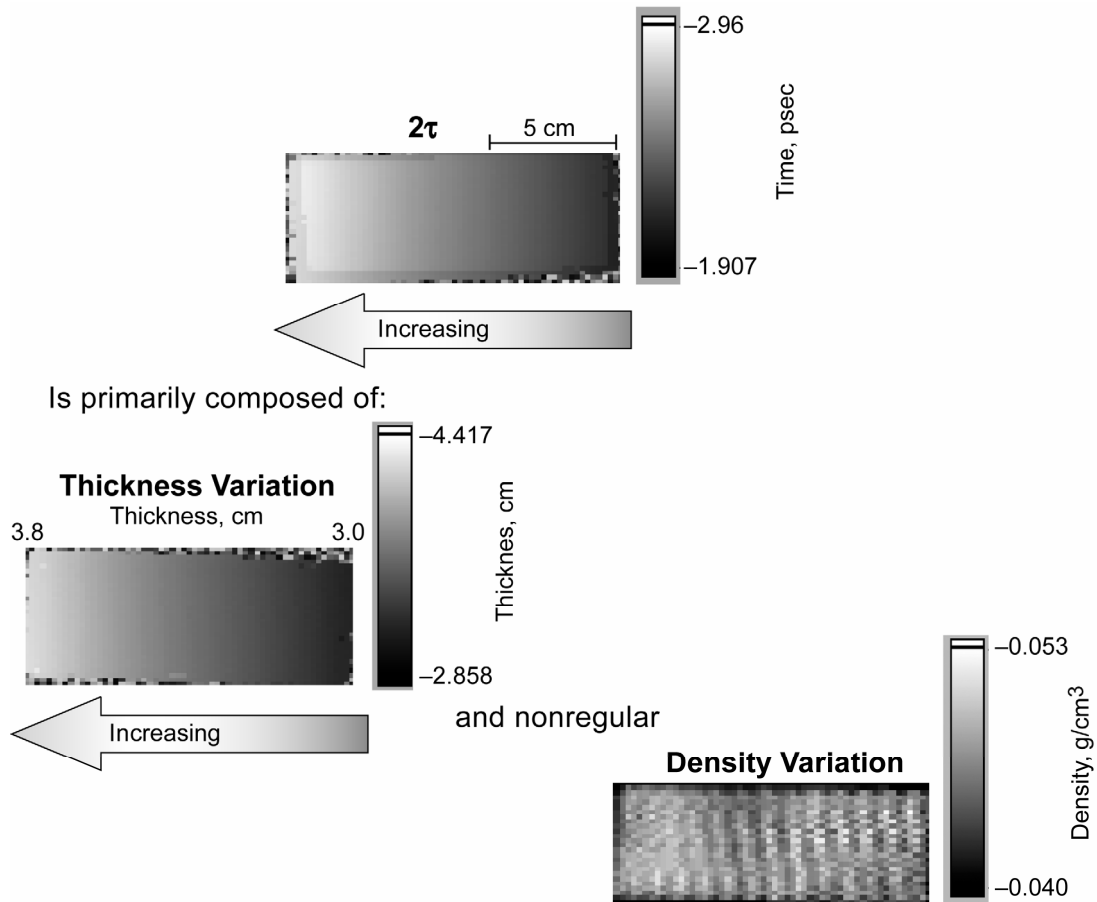


Figure 11.—Results for smooth wedge from terahertz method. Method can be seen to separate out thickness and density effects on time delay (2τ) between *FS* and *BS* echoes. Stitch pattern seen in density image is due to synchronization jitter in scan system and shows prominently due to the small percent variation seen in the velocity image.

density variation is seen for this sample as evidenced by the darker area at the top center versus the surrounding areas in the density image. Thickness measurements taken directly from the thickness image are generally within a few percent of those measured from calipers, although even better agreement was expected as discussed in the MEASUREMENT UNCERTAINTY section.

6 by 15 Foam Block With Nonregular Thickness and Density Variation Pattern

Figure 12 shows a physically-measured density map next to a density map derived from the thickness-independent velocity map obtained using the terahertz method. Viewing lighter and darker areas in the images, it is clear that the physically-measured density variation agrees quite closely with that derived from the thickness-independent velocity.

Figure 13 shows a hand-measured thickness map next to a microstructure-independent thickness map obtained using the terahertz method. Excellent agreement is seen between physical measurement of thickness and thickness obtained from the terahertz method.

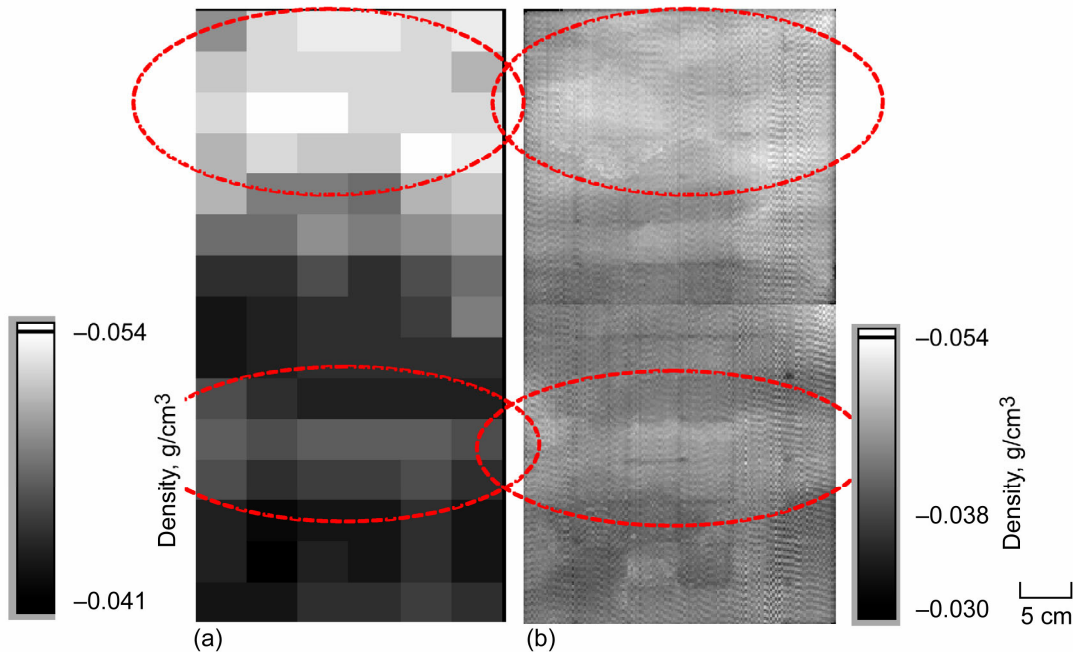


Figure 12.—(a) Physically-measured density (g/cm^3) map for 6 by 15 set of foam blocks and (b) terahertz density map derived from thickness-independent velocity using relationship between terahertz velocity and density for foam shown in figure 2(a). Note excellent correlation between light areas in density maps as denoted by dashed ellipses.

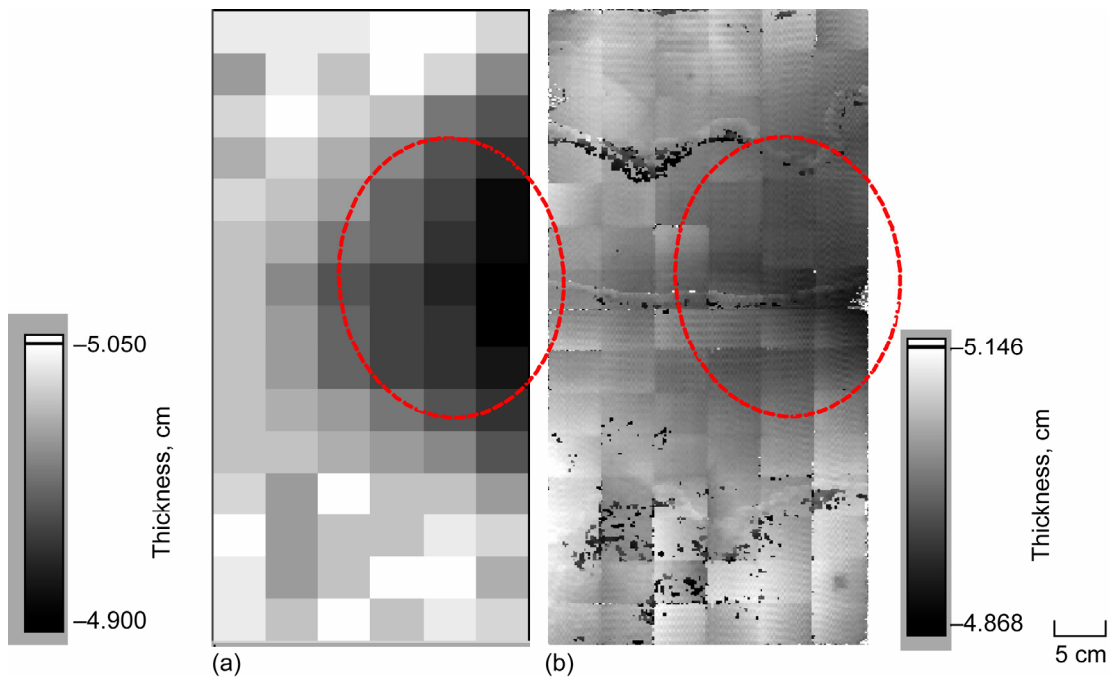


Figure 13.—(a) Hand-measured thickness (cm) map for 6 by 15 set of foam blocks and (b) terahertz microstructure-independent thickness (cm) image for 6 by 15 set of foam blocks. Note excellent correlation between dark and light areas in both images. Dashed ellipse denotes dark areas in both images. Dark scatter spots in microstructure-independent thickness image are due to the presence of an additional echo within the signal processing gate that results in improper cross-correlation delay calculation. This additional echo is likely due to the presence of extra material on the surface. These scatter spots are also in the thickness-independent velocity image of figure 12 but blend better as they cause variation in that image in the same “direction” as actual velocity variations.

Silicon Nitride Ceramic Sample With Known Thickness and Density Variation Pattern

Figure 14 shows a typical fused wavetrain from the processing of waveforms from the silicon nitride sample. The *FS* echo has not been conditioned or amplified in any way indicating a larger dielectric mismatch between this sample and air versus that for foam and air.

Figure 15 shows 2τ , microstructure-independent thickness, and density images for the silicon nitride sample. The density image was derived from thickness-independent velocity image using relationship between terahertz velocity and density for silicon nitride shown in figure 2(b). This sample has well-

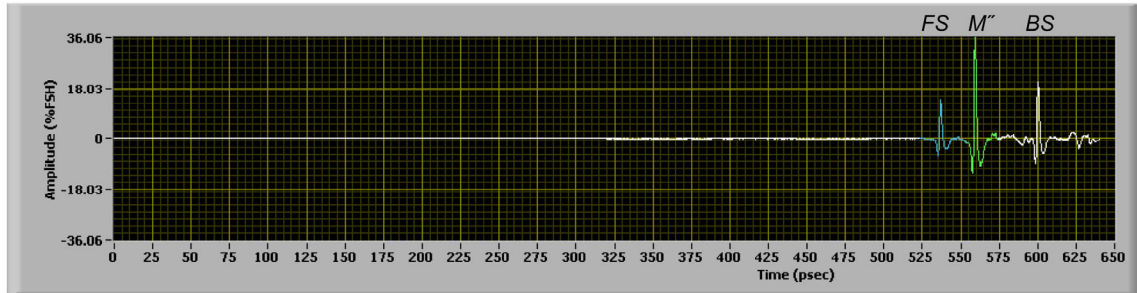


Figure 14.—A typical “fused” waveform from “fused” data file produced by merging the *FS*, *BS*, and *M'* scan data sets for silicon nitride ceramic wedge. No additional conditioning of *FS* was needed for the silicon nitride wedge sample since a reasonably large terahertz reflection off of the silicon nitride surface was obtained.

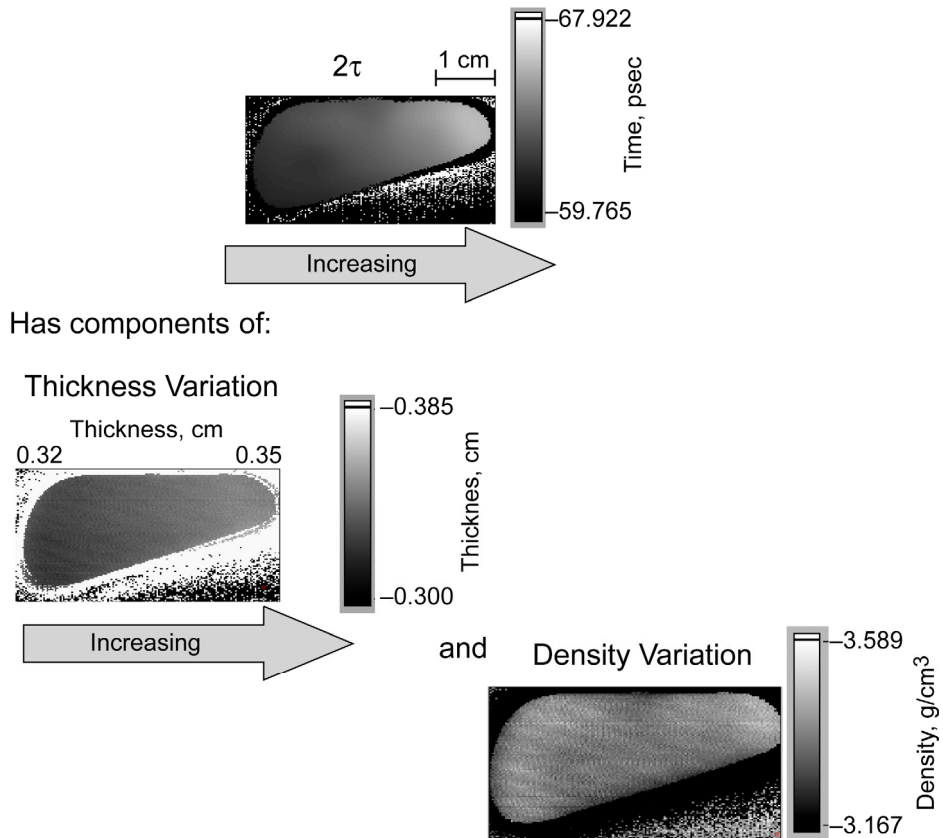


Figure 15.—Results from terahertz method for Silicon Nitride ceramic sample. Method can be seen to separate out thickness and density effects on time delay (2τ) between *FS* and *BS* echoes. Density map was derived from thickness-independent velocity map using relationship between terahertz velocity and density for silicon nitride shown in figure 2(b).

defined thickness and density variation. It can be seen that the method is able to separate the thickness and density variation components. The density variations correspond to those seen optically in figure 6(b). The 2τ image is dominated by the thickness variation but some regional variation indicative of the density variation is noted. Thickness measurements taken directly off of the thickness image are in excellent agreement with those measured using calipers. This is likely due to the high quality *FS* echo and low uncertainty in the process as described in the MEASUREMENT UNCERTAINTY section.

Summary and Significance

This article describes a noncontact single-sided terahertz electromagnetic measurement and imaging method that simultaneously characterizes microstructural (egs. spatially-lateral density) and thickness variation in dielectric (insulating) materials. The method was demonstrated for two materials—Space Shuttle External Tank sprayed-on foam insulation and a silicon nitride ceramic. With high signal-to-noise ratio echoes, the method is very precise as was shown experimentally and through error analysis. Specialized signal processing methods are required to improve the signal-to-noise ratio of front surface echoes off of foam. In this investigation, a wavelet denoising process followed by software amplification were used to make front surface reflections off of the foam usable for this method. A thin layer of plastic can be placed on the foam surface to increase dielectric mismatch and initially locate the front surface echo (so to know the time range to gate).

The method can have significant applicability to characterization of density variations and crushed foam detection for the sprayed on foam insulation of the thermal protection system for the space shuttle external tank. As such, it supports the Columbia Accident Investigation Board recommendation to initiate an aggressive program to eliminate foam shedding. Additional application would be for dielectric materials needing precision density and thickness characterization in a nondestructive fashion. Scale-up to curved/cylindrical shapes, and determination of practical limit of thickness variation, are left for further investigation.

References

1. Altan, H., Huang, F., Federici, J.F., Lan, A., and Grebel, H., "Characteristics of Nano-scale Composite Materials using THz spectroscopy," *Proc. SPIE* **5268**, pp. 53–60, (2004).
2. Arnone, D.D.; et al. Application of terahertz (THz) technology to medical imaging. In *Proc. SPIE Terahertz Spectroscopy Applications II; International Society for Optical Engineering*: Bellingham, WA, 1999; pp. 209–219.
3. Bashyam, M.: Thickness Compensation and Dynamic Range Improvement for Ultrasonic Imaging of Composite Materials. *Proc. Of the 17th Annual Review of Progress in Quantitative Nondestructive Evaluation*, La Jolla, CA, July 15–20, 1990. vol. 10A. Plenum Press, 1991, pp. 1035–1042.
4. Bevington, R.P., **Data Reduction and Uncertainty Analysis for the Physical Sciences**, Chapter 4, 1969. McGraw-Hill, New York, NY.
5. Columbia Accident Investigation Board (CAIB) Report, volume 1, August 2003.
6. Dayal, V. "An Automated Simultaneous Measurement of Thickness and Wave Speed by Ultrasound," *Experimental Mechanics*, 32(3), pp. 197–202, 1992.
7. Generazio, E.R., Roth, D.J., and Stang, D.B.: "Ultrasonic Imaging of Porosity Variations Produced During Sintering," *J. Am. Ceram. Soc.* vol. 72, no. 7, 1989.
8. Hu, B.B. and Nuss, M.C., "Imaging with terahertz waves," *Opt. Lett.*, vol. 20, p. 1716 (1995).
9. Hsu, D.K., et al.: Simultaneous determination of ultrasonic velocity, plate thickness and wedge angle using one-sided contact measurements. *NDT&E International* 1994 vol. 27, no. 2, pp. 75–82.
10. Hull, D.R.; Kautz, H.E.; and Vary, A.: Measurement of Ultrasonic Velocity Using *FS*-Slope and Cross-Correlation Methods. *Mater. Eval.*, vol. 43, no. 11, 1985, pp. 1455–1460.

11. Jensen, A. and la Cour-Harbo, A.; **Ripples in Mathematics**. 157–160. (2001). Berlin: Springer, ISBN 3-540-41662-5.
12. Mittleman, D.M., Jacobsen, R.H., and Nuss, M.C., “T-ray imaging,” *IEEE J. Sel. Top. Quant. Elec.*, vol. 2, p. 679 (1996).
13. Mittleman, D.M., Gupta, M., Neelamani, R.G., Baraniuk, J.V., Rudd and Koch, M., “Recent advances in terahertz imaging,” *Appl. Physics. B* vol. 68. pp. 1085–1094 (1999).
14. NASA Engineering and Safety Center (NESC) External Tank (ET) Thermal Protection System (TPS) NDE Super Problem Resolution Team (SPRT) Final Report, 2007.
15. Piche, L.: Ultrasonic velocity measurement for the determination of density in polyethylene. *Polymer Engineering and Science*, vol. 24, no. 17, Mid-December 1984, pp. 1354–1358.
16. Roth, D.J., Stang, D.B., Swickard, S.M., DeGuire, M.R., and Dolhert, L.E. “Review, Modeling and Statistical Analysis of Ultrasonic Velocity-Pore Fraction Relations in Polycrystalline Materials,” *Materials Evaluation*, vol. 49, no. 7, July 1991, pp. 883–888.
17. Roth, D.J., Hendricks, L., Whalen, M.F. and Martin, K.: Commercial Implementation of Ultrasonic Velocity Imaging Methods via Cooperative Agreement Between NASA—Lewis Research Center and Sonix, Inc. NASA TM–107138, 1996.
18. Roth, D.J., Kiser, J.D., Swickard, S.M., Szatmary, S., and Kerwin, D. “Quantitative Mapping of Pore Fraction Variations in Silicon Nitride Using an Ultrasonic Contact Scan Technique,” *Research in Nondestructive Evaluation*, vol. 6, no. 3, 1995.
19. Roth, D.J., “Using a Single Transducer Ultrasonic Imaging Method to Eliminate the Effect of Thickness Variation in the Images of Ceramic and Composite Plates,” *Journal of Nondestructive Evaluation*, vol. 16, no. 2, June 1997.
20. Roth, D.J., Carney, D.V., Baaklini, G.Y., Bodis, James R., Rauser, Richard W., “A Novel Method for Nondestructive Characterization of Tubular and Curved Components,” *Materials Evaluation*, vol. 56, no. 10, September 1998, pp. 1053–1061.
21. Roth, D.J. and Farmer, D.A., “Thickness-Independent Ultrasonic Imaging Applied to Abrasive Cut-off Wheels: An Advanced Aerospace Materials Characterization Method for the Abrasives Industry; A NASA Lewis Research Center Technology Transfer Case History,” *Materials Evaluation*, vol. 58, no. 4, April 2000.
22. Roth, D.J., Seebo, J.P. Trinh, L.B., Walker, J.L., Aldrin, J.C., “Signal processing approaches for terahertz data obtained from inspection of the shuttle external tank thermal protection system foam,” *Proceedings of the 33rd Annual Review of Progress in Quantitative Nondestructive Evaluation*. Hilton Portland & Executive Tower Portland, Oregon July 30—August 4, 2006.
23. Seebo, J.P., Lockheed-Martin, Inc., Private Discussions.
24. Sollish, B.D.: Ultrasonic Velocity and thickness gage, United States Patent No. 4,056,970, Nov. 8, 1977.
25. Trinh, L., Lockheed-Martin, Inc., Private Discussions.
26. Winfree, W.P. and Madaras, E.I., “Detection and Characterization of Flaws in Sprayed on Foam Insulation with Pulsed Terahertz Frequency Electromagnetic Waves,” *Proceedings of the 41st AIAA/ASME/SAE/ASEE Joint Propulsion Conference & Exhibit*, Tuscon, Arizona, July 10–13, 2005.

REPORT DOCUMENTATION PAGE			Form Approved OMB No. 0704-0188		
<p>The public reporting burden for this collection of information is estimated to average 1 hour per response, including the time for reviewing instructions, searching existing data sources, gathering and maintaining the data needed, and completing and reviewing the collection of information. Send comments regarding this burden estimate or any other aspect of this collection of information, including suggestions for reducing this burden, to Department of Defense, Washington Headquarters Services, Directorate for Information Operations and Reports (0704-0188), 1215 Jefferson Davis Highway, Suite 1204, Arlington, VA 22202-4302. Respondents should be aware that notwithstanding any other provision of law, no person shall be subject to any penalty for failing to comply with a collection of information if it does not display a currently valid OMB control number.</p> <p>PLEASE DO NOT RETURN YOUR FORM TO THE ABOVE ADDRESS.</p>					
1. REPORT DATE (DD-MM-YYYY) 01-03-2008		2. REPORT TYPE Technical Memorandum		3. DATES COVERED (From - To)	
4. TITLE AND SUBTITLE Simultaneous Noncontact Precision Imaging of Microstructural and Thickness Variation in Dielectric Materials Using Terahertz Energy			5a. CONTRACT NUMBER		
			5b. GRANT NUMBER		
			5c. PROGRAM ELEMENT NUMBER		
6. AUTHOR(S) Roth, Don, J.; Seebo, Jeffrey, P.; Winfree, William, P.			5d. PROJECT NUMBER		
			5e. TASK NUMBER		
			5f. WORK UNIT NUMBER WBS 685676.02.99.03.01.01		
7. PERFORMING ORGANIZATION NAME(S) AND ADDRESS(ES) National Aeronautics and Space Administration John H. Glenn Research Center at Lewis Field Cleveland, Ohio 44135-3191			8. PERFORMING ORGANIZATION REPORT NUMBER E-16200		
9. SPONSORING/MONITORING AGENCY NAME(S) AND ADDRESS(ES) National Aeronautics and Space Administration Washington, DC 20546-0001			10. SPONSORING/MONITORS ACRONYM(S) NASA		
			11. SPONSORING/MONITORING REPORT NUMBER NASA/TM-2008-214997		
12. DISTRIBUTION/AVAILABILITY STATEMENT Unclassified-Unlimited Subject Category: 38 Available electronically at http://gltrs.grc.nasa.gov This publication is available from the NASA Center for AeroSpace Information, 301-621-0390					
13. SUPPLEMENTARY NOTES					
14. ABSTRACT This article describes a noncontact single-sided terahertz electromagnetic measurement and imaging method that simultaneously characterizes microstructural (egs. spatially-lateral density) and thickness variation in dielectric (insulating) materials. The method was demonstrated for two materials-Space Shuttle External Tank sprayed-on foam insulation and a silicon nitride ceramic. It is believed that this method can be used as an inspection method for current and future NASA thermal protection system and other dielectric material inspection applications, where microstructural and thickness variation require precision mapping. Scale-up to more complex shapes such as cylindrical structures and structures with beveled regions would appear to be feasible.					
15. SUBJECT TERMS Nondestructive evaluation; Terahertz; Signal processing; Shuttle; External tank; Image processing; Thermal protection system; Foam; Ultrasonic velocity; Thickness					
16. SECURITY CLASSIFICATION OF:			17. LIMITATION OF ABSTRACT UU	18. NUMBER OF PAGES 24	19a. NAME OF RESPONSIBLE PERSON STI Help Desk (email:help@sti.nasa.gov)
a. REPORT U	b. ABSTRACT U	c. THIS PAGE U			19b. TELEPHONE NUMBER (include area code) 301-621-0390

